International Journal for Parasitology 39 (2009) 1319–1330

Contents lists available at ScienceDirect

International Journal for Parasitology

journal homepage: www.elsevier.com/locate/ijpara

An apoptosis-inducing serine protease secreted by the entomopathogenic nematode *Steinernema carpocapsae* ☆

Duarte Toubarro [a], Miguel Lucena-Robles [a], Gisela Nascimento [a], Gonçalo Costa [b], Rafael Montiel [a], Ana V. Coelho [b], Nelson Simões [a,*]

[a] *CIRN, Departamento de Biologia, Universidade dos Açores, Apartado 1422, 9501-801 Ponta Delgada, Portugal*
[b] *ITQB, Universidade Nova de Lisboa, Apartado 127, 2780 Oeiras, Portugal*

ARTICLE INFO

Article history:
Received 2 December 2008
Received in revised form 9 April 2009
Accepted 14 April 2009

Keywords:
Apoptotic factor
Biochemical characterisation
Chymotrypsin
Full-length cDNA
Entomopathogenic nematode
Protein purification
Serine protease

ABSTRACT

Steinernema carpocapsae is an insect parasitic nematode able to parasitise and kill the host within 48 h. Secreted products (ESP) of the parasitic stage of a virulent strain contain higher amounts of proteolytic activity than a low virulence strain, suggesting proteases are involved in virulence. From the ESP we purified a protein (Sc-SP-3) with a M_r of 30 kDa and a p*I* of 7 that cleaved the synthetic substrate N-succinyl-Ala-Ala-Pro-Phe-pNA and was inhibited by phenylmethanesulfonyl fluoride, benzamidine and chymostatin, thus indicating that it belongs to the chymotrypsin-like serine protease family. Sc-SP-3 has a V_{max} of 0.3 mM min^{-1} ml^{-1} and K_m of 6.6×10^{-4} M, with maximum activity at pH 8 and 40 °C. The full-length cDNA was obtained using degenerate oligonucleotides for serine proteases. This open reading frame encodes a preproprotein containing a putative signal peptide composed of 16 amino acid residues, a prodomain of 40 residues and a mature protease domain of 261 residues, including the catalytic triad His/Asp/Ser characteristic of trypsin-like serine proteases. The N-terminal sequence and the peptide masses fingerprint obtained by MALDI-TOF–MS for the purified protein matched the cDNA. Gene expression analysis by quantitative real-time-PCR showed that this gene is expressed only during the parasitic stage and that pre-invasive nematodes inside the mid-gut expressed higher amounts of Sc-SP-3 than those that already enter the haemocoel. Sc-SP-3 caused histolysis in the insect mid-gut. In vitro assays demonstrated that Sc-SP-3 digested extracellular proteins and induced apoptosis in *Sf*9 insect cells, thus suggesting Sc-SP-3 is a multifunctional chymotrypsin-like protease involved in pathogenesis.

1. Introduction

Steinernema carpocapsae is an insect parasitic nematode that forms a symbiotic association with the bacterium *Xenorhabdus nematophila*. Because of its high virulence, it is used to control several insect pests and vectors (Kaya and Gaugler, 1993). Nematode infective juveniles (IJs) are resistant stages living in the soil, where they seek suitable hosts. Host contact induces the nematode parasitic stage via recovery of IJs (Forst and Clarke, 2002). The recovered nematodes are able to invade, establish themselves in the general cavity of the insect and kill their host. After entering the insect, which occurs mostly through the mouth and anus, nematodes must overcome the host's natural barriers – including the peritrophic membrane, intestinal wall and adjacent tissues and invade the insect haemocoel in order to become established. Although the mechanisms involved in this process remain unknown, 50% of *Galleria mellonella* larvae exposed to IJs become infected after 12 h, demonstrating the high ability of these nematodes to invade insects.

The establishment of a parasite in a host depends greatly on its ability to manage host defenses (Else, 2005). Evasion seems to be a generalised feature of *S. carpocapsae*, despite a few exceptions such as humoral encapsulation, as observed for the dipteran *Tipula oleraceae* (Peters and Ehlers, 1997), and cellular encapsulation for the lepidopteran *Pseudalaetia unipuncta* (Cruz et al., 2001). Evasion must result from either the ability of the nematode to actively destroy cellular and humoral insect defense mechanisms or its capacity to mimic insect recognition. Gotz et al. (1981) showed that *S. carpocapsae* was able to destroy antibacterial peptides and thus deplete the insect's defenses. Wang and Gaugler (1999) attributed the nematode's ability to mimic insect recognition of specific proteins expressed in the epicuticle of the invasive IJs.

The *S. carpocapsae–X. nematophila* complex is highly pathogenic to insects. *G. mellonella* larvae exposed to the nematode IJs are killed approximately 38 h post-exposure. Mortality is attributed mainly to virulence factors produced by the associated bacteria, including toxins (Sergeant et al., 2003), proteases (Caldas et al.,

☆ *Note:* Nucleotide sequence data reported in this paper are available in the GenBank™ database under the Accession No. FJ152416.

* Corresponding author. Tel.: +351 296 650 119; fax: +351 296 650 100.
E-mail address: simoes@uac.pt (N. Simões).

0020-7519/$36.00 © 2009 Australian Society for Parasitology Inc. Published by Elsevier Ltd. All rights reserved.
doi:10.1016/j.ijpara.2009.04.013

2002) and lipases (Thaler et al., 1998). However, the same lethality time was observed for insects exposed to axenic *S. carpocapsae* (Laumond et al., 1989), suggesting that the parasitic nematode is also able to produce insecticidal factors. Lethal factors have been detected in insects parasitised with axenic *S. carpocapsae* (Boemare et al., 1982), as well as in the culture medium of axenic nematodes (Burman, 1982). Furthermore, analysis of excreted–secreted products (ESP) from the parasitic stage of *S. carpocapsae* showed the presence of a large number of different proteins and distinct activities, namely cytotoxicity, proteolysis and immunosuppression. Proteolytic activity has been shown to be higher in ESPs from a virulent strain than in that from a less virulent strain (Simões et al., 2000).

Proteases, apoptosis-inducing factors and other active compounds had been suggested to be actively secreted/excreted by parasitic nematodes into host tissues (James and Green, 2004). Proteases deployed by parasitic nematodes must participate in some of the tasks imposed by the parasitic lifestyle, including invasion, digestion of host tissues and evasion of host immune responses (Sakanari and McKerrow, 1990). Serine proteases are among the most representative compounds in nematodes ESPs, which also include cysteine, metallo and aspartic proteases (Trap and Boireau, 2000). In *Schistosoma mansoni*, secreted serine proteases are mostly associated with degradation of the extracellular matrix, thus ensuring host penetration (McKerrow et al., 1985). Cysteine proteases are present in *S. mansoni* and have been suggested to participate in nutrition (Smith et al., 1994); in *Fasciola hepatica* it has been suggested they aid parasitic penetration and host tissue degradation (Berasain et al., 1997); and in *Taenia solium* they were described to have a potential role in evasion of host defense mechanisms (McKerrow et al., 1985). Metalloproteases related to nutrition have been identified in *Haemonchus contortus* (Redmond et al., 1997) and have been found to participate in evasion in *T. solium* (White et al., 1992). Aspartic proteases identified in *S. mansoni* were suggested to be involved in nutrition (Wong et al., 1997), whereas in *T. solium* they were related to evasion (White et al., 1992).

A few parasites may use host cell apoptosis as a survival strategy to establish infection in their host by creating around them an immune-privileged site (Rahman and McFadden, 2006). *Brugia microfilariae* secrete a factor that activates CD4+ T cells to indirectly trigger apoptosis in lymphocytes (Jenson et al., 2002); *S. mansoni* secretes a 23 kDa protein with proapoptotic activity that apparently is mediating the Fas/FasL pathway (Chen et al., 2002); and *Nippostrongylus brasiliensis* releases bioactive molecules that were understood to trigger apoptosis in intestinal epithelial cells through up-regulation of the death receptor protein Fas (Kuroda et al. 2002). *Trichuris muris* was described to promote an infection process which triggers apoptosis in intestinal epithelial cells (Cliffe et al., 2007).

In the present work, we purified and characterised a serine protease that was identified in the ESP of the parasitic stage of the entomopathogenic nematode *S. carpocapsae*. We cloned and sequenced the full-length cDNA encoding this protein and demonstrated that this protease has multifunctional activity that results in hydrolysis of extracellular matrix proteins and induces apoptosis.

2. Materials and methods

2.1. Nematode secreted products

Steinernema carpocapsae Breton strain was multiplied in vitro according to Bedding (1984). IJs were stored in tap water at 10 °C for 2–4 months before use in assays. To obtain ESPs, recovery of IJs was induced in vitro by adding insect tissue homogenates to the medium. To prevent contamination of ESPs with proteins from insect tissues, we performed a two-step protocol. First, IJs were induced for recovery and then they were carefully washed and transferred to a new saline solution free of insect tissue to obtain the ESP. About 2.5×10^4 IJs were surface sterilised with 0.5% sodium hypochloride, washed three times with 0.8% NaCl solution, transferred to a 90 mm Petri dish in 10 ml of recovery inducing medium composed of Tyrod's medium with 10% heat denatured insect homogenate added with penicillin, streptomycin and neomycin (0.05 mg; 0.1 mg; 50 U) (Sigma) and incubated at 23 °C with agitation for 18 h. Recovered nematodes (parasitic stage) were then washed three times with 0.8% NaCl (w/v) solution plus antibiotics, transferred to a new Petri dish with 10 ml of Tyrod's without insect homogenate and incubated for an additional 3 h. Finally, the nematodes were separated using a 0.22 μm filter to obtain ESPs, which were used for serine protease purification.

2.2. Protease purification

One hundred millilitres of ESPs were concentrated to a final volume of 1 ml using Amicon Ultra 5K (Millipore). Five hundred microlitres of this material was applied to a Superdex 200 gel filtration column (Amersham) equilibrated in 50 mM Tris–HCl, pH 7.4, 0.5 M NaCl. Active fractions were pooled and subsequently applied to a 1 ml HiTrap benzamidine FF (Amersham) equilibrated with the same buffer and eluted in 50 mM glycine buffer at pH 3. Fractions were collected in tubes containing 100 μl of 1 M glycine buffer, pH 9.5, to avoid denaturation. Active fractions were pooled and applied to a Mono Q 5/5 (Amersham) equilibrated with 50 mM glycine buffer at pH 9.5 and eluted using a gradient of 1 M NaCl. All experiments were performed at 4 °C. The soluble protein concentrations were determined at all purification steps using the Qubit Fluorometer (Invitrogen) according to the manufacturer's instructions.

2.3. SDS–PAGE and zymogram analysis

SDS–PAGE was performed with a Mini-protean II gel system (Bio-Rad) using slab gels of 12% polyacrylamide. Samples were dissolved in non-reducing sample buffer (Laemmli, 1970) and run at 100 V. Proteins were colloidal coomassie stained according to Neuhoff et al. (1988). The SDS–PAGE zymogram was performed in 12% polyacrylamide gels co-polymerised with 0.05% gelatin. After electrophoresis, the gels were washed three times for 30 min in 50 mM Tris–HCl buffer, pH 7.6, containing 2.5% Triton X-100. The gels were then incubated for an additional 4 h in a solution of 50 mM Tris–HCl, pH 7.6, containing 0.2 M NaCl and 5 mM $CaCl_2$. Zones of proteolysis were detected by Coomassie blue staining.

2.4. Two-dimensional electrophoretic analysis

The 1 ml fraction from the Mono Q purification step was precipitated with TCA at a final concentration of 30% and centrifuged for 10 min at 10,000*g*. The pellet was dried and resuspended with rehydration buffer (9.8 M urea, 4% cholamidopropyl)dimethylammonio]-1-propanesulfonate (CHAPS) (w/v), 2 mM tributylphosphine solution (TBP) and 0.5% (v/v) 3–10 ampholytes). The sample was loaded into 7-cm ready strips (Bio-Rad) and actively re-hydrated for 12 h at 20 °C according to the manufacturer's instructions. The strips were focused in three steps: S_1, 250 V for 15 min; S_2, 250–4,000 V for 2 h; and S_3, 4,000 V for 5 h. Prior to two-dimensional (2D) analysis the strips were equilibrated in a solution of 6 M urea, 2% (w/v) SDS, 0.375 M Tris–HCl, pH 8.8, 20% (w/w) glycerol and 0.130 M DTT for 10 min and then alkylated in a solution of 6 M urea, 2% SDS 0.375 M Tris–HCl, pH 8.8,

20% glycerol and 0.135 M iodoacetamide for 10 min. SDS–PAGE was performed in 1.5-mm-thick 12% acrylamide gel under the conditions described above.

2.5. Analysis of specific substrates and inhibitors

To determine its specific substrate, the purified protease was assayed for proteolytic activity using several substrates (see Table 1). Ninety microlitres of purified protein (30 μg/ml) was homogenised in 10 μl of each colorimetric substrate at a final concentration of 1 mM in a 96-well plate. The absorbance was read at 405 nm in a microplate reader (Bio-Rad) and readings were taken every 45 s. One unit of activity corresponds to the difference between two consecutive readings inside the exponential curve multiplied 100 times. To assay specific inhibitors, the purified protease was tested with N-succinyl-Ala-Ala-Pro-Phe-pNA substrate in the presence of different protease inhibitors (see Table 2). Hydrolysis was measured as described above.

2.6. Kinetic analysis

Kinetic assays were performed using N-succinyl-Ala-Ala-Pro-Phe-pNA as substrate. The reaction mixture contained 3 μg of *Steinernema carpocapsae* serine protease-3 (Sc-SP-3), and substrate concentrations ranged from 0.1 to 2.4 mM in a final volume of 90 μl. Reactions were performed in triplicate. Activity was measured as described above. V_{max} and K_m values were determined using the Lineweaver–Burk plot.

2.7. Determination of optimal pH and temperature

The reactivity of the purified protease was assayed in triplicate in the presence of N-succinyl-Ala-Ala-Pro-Phe-pNA substrate prepared in buffers with pH values ranging from 4 to 11. Controls consisted of substrate solution at the same pH but without the protease. To determine optimal temperature, reactions were performed in triplicate at optimal pH, with temperatures ranging from 5 to 55 °C, for 5 min. Proteolytic activity was measured as described above.

2.8. Preparation for N-terminal amino acid sequencing

A chromatographic purified fraction of protease was subjected to 2D electrophoresis and electroblotted onto polyvinylidene pifluoride membranes (PVDF) membrane (Millipore). Two millimolar Tris, 192 mM glycine, 20% methanol and 0.2% SDS, pH 8.3, was used as the electrophoretic buffer in a Mini Trans-Blot Cell (Bio-Rad). The protease present on the PVDF membrane was stained with a solution of 0.5% Ponceau Red, washed with water, excised and subjected to analysis. N-terminal amino acid sequence analysis was performed using automated Edman degradation by the Emory Microchemical Facility (Atlanta, GA, USA).

Table 1
Activity of purified *Steinernema carpocapsae* serine protease-3 in specific substrates.

Substrate	Activity (U)
N-succinyl-Ala-Ala-Pro-Phe-pNa	240
N-benzoyl-Gly-Phe-pNa	24
N-methoxysuccinyl-Ala-Ala-Pro-Met-pNa	20
N-succinyl-Ala-Ala-Pro-Leu-pNa	20
N-succinyl-Gly-Gly-Phe-pNa	10
Ala-Ala-Phe-p-Na	10
N-benzoyl-Pro-Phe-Arg-pNa hydrochloride	8
Z-Gly-Gly-Leu-pNa	0
N-benzoyl-L-tyrosine	0
N-benzoyl-Phe-Val-Arg-pNa hydrochloride	0

Table 2
Inhibition rate of *Steinernema carpocapsae* serine protease-3 activity in N-succinyl-Ala-Ala-Pro-Phe-pNA by specific inhibitors.

Inhibitor	Inhibition (%)
Benzamidine	100
PMSF	100
Chymostatin	70
STI	50
TPCK	40
Phenanthroline	30
Antithrombin III	12
Aprotinin	10
Phosphoramidon	0
E64	0
EDTA	0
Leupeptin	0
Pepstatine	0

PMSF, phenylmethanesulfonyl fluoride; STI, soybean trypsin inhibitor; TPCK, Nptosyl-L-phenylalanine chloromethyl ketone; E64, *trans*-epoxysuccinyl-L-leucylamido(4-guanidino)butane; EDTA, ethylenediaminetetraacetic acid tetrasodium salt.

2.9. MALDI-TOF–MS analysis

MALDI-TOF–MS analysis was performed in a single spot excised from the polyacrylamide gel of the 2D electrophoresis after being dehydrated using a speed vacuum and re-hydrated with 6.7 μg/ml of sequencing grade trypsin (Promega) in 50 mM ammonium carbonate buffer, pH 8, for 30 min. The excess of buffer was discarded, 20 μl of ammonium carbonate buffer was added and the sample was incubated for 16 h at 37 °C. The digested peptides were concentrated and desalted using a microcolumn Poros R2 and directly eluted into a MALDI plate using α-cyano-4-hydroxycinnamic acid (CHCA) in 70% (v/v) acetonitrile with 0.01% (v/v) trifluoracetic acid.

Monoisotopic masses of Sc-SP-3 were obtained using a MALDI-TOF–MS model Voyager-DE-STR (Applied Biosystems). External mass calibration was performed using a mixture of peptide standards, PepMix1 (Laserbio Labs). The *m*/*z* masses were used to search in NCBI non-redundant protein database (www.ncbi.nlm.nih.gov), using the internet public version of Mascot software (www.matrixscience.com) thus allowing for peptide mass fingerprint identification. Trypsin digestion, a maximum of one missing cleavage, a cysteine carbamidomethylation and the possibility of methionine oxidation were selected as conditions.

2.10. Real-time-PCR and 5′–3′ RACE

To obtain RNA, recovered nematodes were powdered in liquid nitrogen and stored at −80 °C until analysis. RNA was isolated with TRIzol (Invitrogen), and first-strand cDNAs were generated using 0.2 μg of total RNA and a p(dT)-anchor primer, 5′-GGGGCGGC CGC$(T)_{30}$-3′, with the SuperScript™ First-strand synthesis system for RT-PCR (Invitrogen) according to the manufacturer's instructions. PCR amplifications were performed using the degenerate primer TCSP (5′-TIACNGCIGCICAYTGYKT-3′) based on conserved motifs present beside the catalytic histidine of serine proteases (His57, following the bovine chymotrysinogen numbering system) and the p(dT)-anchor primer. Samples were subjected to an initial denaturation step at 94 °C for 5 min, followed by touchdown PCR cycling as follows: 94 °C for 30 s; 10 cycles of 63 °C for 60 s with a decrease of 1 °C per cycle; and 72 °C for 180 s; followed by 25 similar cycles with an annealing temperature maintained at 54 °C and an elongation time of 120 s, with a final elongation step at 72 °C for 10 min. The 5′-end of the cDNA fragment derived from the RT-PCR was amplified by 5′ rapid amplification of cDNA ends using the SMART™ RACE cDNA Amplification Kit (Clontech). The anti-sense primers, 5R209 (5′-CGGCGTCGTCCTCGACAATCTTTGTGAG-3′) and

5R819 (5′-GAATTCGTCGTCGAATTTGTC-3′), were used for the first and second rounds of the PCR, respectively. The conditions for the first round of PCR were a denaturation step at 94 °C for 5 min; five cycles of 94 °C for 5 s, 72 °C for 10 min and 72 °C for 180 s; five cycles of 94 °C for 5 s, 70 °C for 10 s and 72 °C for 180 s; 25 cycles of 94 °C for 5 s, 68 °C for 10 s and 72 °C for 180 s; and a final elongation at 72 °C for 10 min. The same conditions were used in the second round of PCR, except that the annealing temperature was decreased from 58 to 54 °C. The authenticity of the cDNA sequences were confirmed by 3′-RACE using the sense primers, 3R196 (5′-CCGCGACGTCCAGC TCACAAAGATTGTC-3′) and 3R415 (5′-AGCTACAACTCGCATACACT AC-3′). PCR amplifications were performed as above, except that the annealing temperature in the second round of PCR was decreased from 60 to 56 °C.

2.11. DNA sequencing and sequence analysis

The amplified cDNA fragments were cloned into pCR4-TOPO vector using the TOPO TA Cloning® Kit for sequencing (Invitrogen). Plasmid clones were sequenced in both directions using T3 and T7 primers with the PRISM® Dye Terminator Cycle Sequencing System (Applied Biosystems) and an automated capillary electrophoresis sequencer. Nucleotide and amino acid sequence analysis was carried out using the CLUSTAL W (http://www.ebi.ac.uk/clustalw/) and the sequences obtained were used as queries in BLAST searches of GenBank at the National Center for Biotechnology Information (http://www.ncbi.nlm.nih.gov), the *Caenorhabditis elegans* genome at WormBase (http://www.wormbase.org), and the MEROPS protease database at the Wellcome Trust Sanger Institute (http://merops.sanger.ac.uk). Signal sequence cleavage site prediction was performed using the SignalP software (Nielsen et al., 1997). Domains were predicted with Smart software (http://smart.embl-heilderberg.de/smart).

2.12. sc-sp-3 expression during the nematode life cycle

sc-sp-3 expression throughout the nematode life cycle into parasitised insects was investigated by quantitative real-time-PCR. Chilled *G. mellonella* larvae were dissected post-exposure to IJ in order to harvest nematodes representing each stage of the life cycle. IJs that had not invaded insect haemocoel were harvested in the mid-gut at 7 h post-exposure (PE) and IJs that had already penetrated haemocoel were collected 18 h PE from the haemocoel. Fourth stage, adults, and first and second stage were harvested later, after inspection of parasitised insects for the desired nematode developmental stage. Ten nematodes in each stage were washed three times, transferred to lysis buffer for RNA extraction and purification using the RNeasy Micro Kit (QIAGEN). The data represent at least three independent experiments. Reverse transcription was performed using Superscript first-strand III (Invitrogen) with random primers. Quantification of *sc-sp-3* expression in relation to 18S rRNA was performed using SYBR green master mix (Applied Biosystem) with a Real-Time thermocycler AB 7900HT and specific primers for *sc-sp-3*: sense 5′-TGTTGCTCAGGACGGGAAAG-3′; antisense 5′-CACAGAAGTAGGACGTGCGAAG-3′; and for 18S: sense 5′-AAACGAAAGTCTTCCGGTTCC-3′; anti-sense 5’-GGGTGAGTTTTC CCGTGTTG-3′.

2.13. Histology

Fourth instars of *G. mellonella* larvae were fed with 0.1 mg of purified protease imbibed in 2% agar coloured with blue food dye. Twenty four hours later larvae that presented with a blue mid-gut, indicating they had fed on protease, were dissected after chilling to excise the fixed mid-gut. Ex vivo mid-gut was prepared from healthy fourth instars of *G. mellonella*. Excised mid-gut was sectioned transversely into 4-mm thick pieces under sterile conditions. Each piece was transferred to 50 μl of Grace’s medium plus penicillin–streptomycin–neomycin (0.05 mg; 0.1 mg; 50 U) (Sigma) at a final concentration of 30 μg/ml of purified protein and incubated for 3 and 6 h at room temperature. Entire mid-gut and mid-gut pieces were then fixed in Carnoy for 12 h, dehydrated in a gradient ethanol series and embedded in paraffin. Seven-micron-thick serial sections were obtained and stained with Mayer’s haemalum and eosin.

2.14. Tissue homogenate and extracellular protein assays

Mid-gut was excised from dissected *G. mellonella* larvae, powdered in liquid nitrogen, homogenised using a mortar and centrifuged at 10,700*g* for 30 min at 4 °C, and the supernatant was stored at −80 °C until use. To analyse the activity of Sc-SP-3, 3 μg of purified protease was incubated with 20 μg of tissue protein extract in 0.1 M Tris–HCl, pH 8, for 2 h at 27 °C. Protease activity was also tested against the extracellular proteins fibronectin, collagen and laminin (Sigma) by incubating 3 μg of purified protease with 10 μg of each protein in 20 μl of 0.1 M Tris–HCl, pH 8, under the conditions previously described. Profiles of treated and non-treated proteins were obtained in a 5–20% gradient SDS–PAGE for comparison.

2.15. Cell toxicity and apoptosis assays

Spodoptera frugiperda cells (*Sf*9) (Invitrogen) are currently maintained in our laboratory in Sf-900 II SFM medium supplemented with L-glutamine and the antibiotics penicillin, streptomycin and neomycin (0.05 mg; 0.1 mg; 50 U) (Sigma). Confluent cells with >95% viability, as assessed by the Trypan blue exclusion test, were used in all experiments. Cytotoxic assays were conducted in 96-well plates seeded with 1×10^5 cells per well and incubated with different concentrations of Sc-SP-3 and for different times at 27 °C. Positive controls were done with EGTA 50 mM. To test cytotoxicity, 0.5 mg/ml of yellow tetrazolium salt (MTT) was added to each well of the treated cells and incubated for 3 h. The supernatant was removed and the formazan crystals dissolved in DMSO. Cell mortality was determined by subtracting the absorbance values measured at 690 nm from that measured at 572 nm. To assess DNA fragmentation, treated cells were washed twice with PBS, suspended in 200 μl of lysis buffer (100 mM NaCl, 10 mM Tris–HCl, pH 7, 25 mM EDTA, 0.5% (w/v) SDS) containing 0.3 mg/ml of proteinase K, and incubated at 55 °C for 12 h. The homogenate was then digested with 1 mg/ml of RNase A for 1 h at 37 °C and the DNA extracted with an equal volume of phenol/chloroform/isoamyl alcohol. The extracted DNA was precipitated with ethanol, dissolved in Tris–EDTA buffer (TE) and loaded in a 1.2% (w/v) agarose gel. A 100 bp standard marker was used in each electrophoresis.

Caspase activity in cells was determined using N-acetyl-Asp-Glu-Val-Asp p-nitroanilide (DEVD-pNA) hydrolysis in the cell extracts according to colorimetric protease assay sampler Kit (Invitrogen). Approximately 400 μg of extract protein was taken in 50 μl of extract buffer and diluted with 20 mM Tris–HCl (pH 7.2) to obtain 100 μg protein in 50 μl. Prepared protein extract was diluted (1:1) in reaction buffer containing 1 mM DTT and DEVD-pNA was added at 10 μM final concentration. The mix was incubated at 37 °C and DEVD-pNA hydrolysis was monitored by spectrometry at 405 nm excitation. Caspases inhibition was done following Aparna et al. (2003); in brief *Sf*9 cells were pre-incubated for 30 min with 50 μM of cell-permeable z-VAD-fmk caspase inhibitor (Sigma) and then treated with Sc-SP-3 as before.

For microscopy, the cells were grown in 12-well plates on a coverslip treated with poly-L-lysine to promote cell attachment and incubated at 27 °C for 24 h. Confluent cells were treated with

30 μg/ml of Sc-SP-3 for 18 h. Nuclear fragmentation was analysed using DAPI (Sigma). The rate of mortality represents a mean of five microscopy fields. Treated cells were fixed with 4% (v/v) paraformaldehyde in PBS for 20 min, rinsed and permeabilised with 0.1% (v/v) Triton X-100 in PBS for 15 min. The cells were washed two more times with PBS and stained with 20 μg/ml of DAPI for 10 min at 27 °C. Finally, the cells were washed with PBS and observed under a fluorescence microscope (Zeiss) at 350 nm. To analyse plasma membrane integrity and surface exposed phosphatidylserine, treated cells were incubated with FITC-conjugated annexin-V and propidium iodide in binding buffer using the Apoptosis Detection Kit (Invitrogen). Living cells were visualised using Hoechst 33342 (Sigma) at 5 μg/ml. Active caspase was detected in monolayer *Sf*9 cells using a mammalian caspase 3 antibody (Cell Signalling Technology) that had been used to study caspase homologues in *S. littoralis* (Vilaplana et al., 2007). In brief, treated and control cells were fixed in 4% paraformaldehyde, permeabilised with 0.5% (v/v) Triton X-100 in PBS, the peroxidases were blocked with 3% (v/v) H_2O_2 in PBS and then incubated with caspase antibody for 24 h at 4 °C. Detection was performed using the TSA tetramethylrhodamine system (PerkinElmer Life Sciences), according to the manufacturer's instructions. Images were processed using Image Software Elements (Nikon).

3. Results

3.1. Secreted products and protease purification

At 6 h of incubation, recovery of *S. carpocapsae* IJs was confirmed by visualisation of the pumping activity of the esophageal bulb. At this incubation time, in ESPs a few proteins were visualised by SDS–PAGE (data not shown) and proteolytic activity against the specific substrate N-succinyl-Ala-Ala-Pro-Phe-pNA was detected. This activity increased about 3-fold at 12 h and 1.5-fold at 18 h of incubation (Fig. 1). At this time recovered nematodes were transferred to fresh saline solution free of insect tissues to obtain ESPs. No proteolytic activity or proteins were detected in the saline solution immediately after nematode transfer, but were detectable 3 h later, thus indicating that recovered nematodes continued to secrete in the absence of insect homogenate. To purify the protease described herein, the nematodes were separated by filtration and the solution containing ESPs was concentrated.

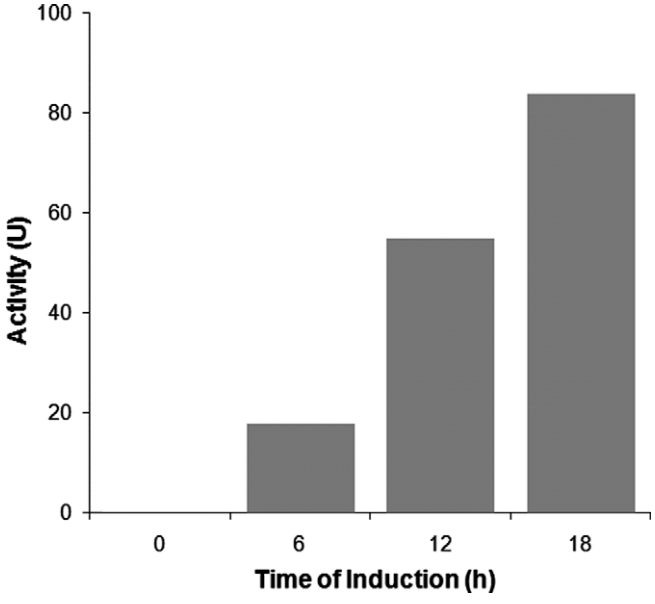

Fig. 1. Proteolytic activity measured in excreted–secreted products (ESPs) of the parasitic stage of *Steinernema carpocapsae* along the time of incubation. Parasitic stage was induced by incubating infective juveniles (IJs) with 10% insect homogenate. Proteolytic activity was tested against the specific substrate N-succinyl-Ala-Ala-Pro-Phe-pNA in aliquots taken at different times. Values are the mean of at least three reactions from different incubation batches.

One hundred millilitres of ESPs containing 11 U/mg of specific proteolytic activity were concentrated to 0.5 ml, reaching a specific activity of 131 U/mg (Table 3). This extract was separated to purification in three successive chromatographies (Fig. 2). In the gel filtration a peak containing 483 U/mg of proteolytic activity was collected with a calculated mass weight of about 30 kDa. Active fractions were pooled and concentrated, and then bound to a serine protease affinity column and eluted with 50 mM glycine, pH 3. A fraction with 1,800 U/mg of specific activity was concentrated, applied to a Mono Q column and eluted with 0.35 M NaCl in a 1 ml fraction with a specific activity of 2,775 U/mg. In this fraction, a single band of protein was visualised in SDS–PAGE, a single band of hydrolysis was observed in the zymogram, and also a single spot with 30 kDa and p*I* of approximately 7 was detected in 2D electrophoresis (Fig. 3).

3.2. Biochemical characterisation

Among the chromogenic substrates analysed for susceptibility to the purified protease, only N-succinyl-Ala-Ala-Pro-Phe-pNA was significantly hydrolysed (Table 1). Proteolytic activity against N-succinyl-Ala-Ala-Pro-Phe-pNA was completely inhibited by benzamidine and PMSF, and 70% by chymostatin (Table 2), indicating that the purified protein was a chymotrypsin-like serine protease. Pure protease was shown to be pH- and temperature-dependent, with maximum activity at pH 8 and 40 °C (Fig. 4). Furthermore, it was thermolabile, demonstrating a loss of activity after treatment for 10 min at 60 °C. Purified protease activity against N-succinyl-Ala-Ala-Pro-Phe-pNA had a V_{max} of 5.0×10^6 Mol min^{-1} ml^{-1} and a K_m of 4.8×10^3 Mol ml^{-1}.

3.3. cDNA sequencing and deduced amino acid sequence analysis

RT-PCR amplification of total RNA from recovered *S. carpocapsae* using a degenerate oligonucleotide surrounding the active His57 site resulted in two distinct bands of approximately 0.80 kb. Sequencing of a number of clones from the mixed PCR products obtained from recovered nematodes revealed different cDNA sequences, and their deduced proteins demonstrated homology with other serine proteases. Three different full-length cDNAs were then identified and isolated by 5′–3′ RACE. Additional RT-PCR reactions were performed with specific primers corresponding to the regions coding for proprotein and mature protein for every cDNA, resulting in the amplification of fragments with the expected size. DNA sequencing of these clones validated the accuracy and authenticity of each cDNA cloned (data not shown). One of these cDNA was designated *sc-sp-3* (*S. carpocapsae* serine protease number 3) and deposited in GenBank under Accession No. FJ152416. *sc-sp-3* is an 1,108 bp cDNA comprising 67 bp in the 5′-UTR, 90 bp in the 3′-untranslated regions (UTR) and an open reading frame of 951 bp. A potential polyadenylation signal (GGTAAA) was also detected.

Sc-SP-3 is a predicted putative 317 amino acid protein that appears to be synthesised as a precursor molecule in a preproform, revealing a putative signal peptide of 16 residues, a prodomain of 40 residues and a mature protease domain of 261 amino acid residues (Fig. 5), with a predicted molecular mass of 28,900 Da. Comparison of the predicted N-terminal sequence of the mature Sc-Sp-3 protease with other serine proteases did not result in the identification of any zymogen activation at residues 56–60

Table 3
Summary of *Steinernema carpocapsae* serine protease- purification in this study.

Sample analysed	Total (mg)	Total act (U)[a]	Sp act (U/mg)[b]	Purification factor
Concentrated SP	3.1	410	131	
Superdex 200	0.6	290	483	3.69
Benzamidine FF	0.15	270	1800	13.7
Mono Q	0.08	222	2775	21.2

[a] One unit of protease activity was defined as the amount of enzyme required to produce an absorbance change of 0.01 absorbance under the condition of the assay.
[b] Sp act, specific activity.

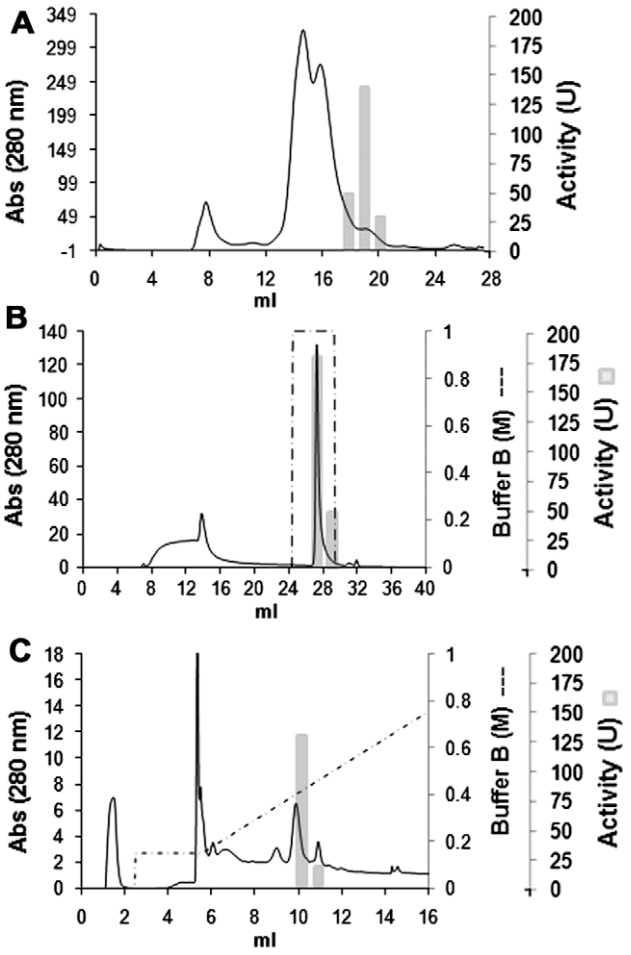

Fig. 2. Purification of *Steinernema carpocapsae* serine protease-3 was obtained passing active material in three successive chromatographies. Profiles obtained in gel filtration (A), Hitrap Benzamidine FF (B) and Mono Q (C), with indication of proteolytic activity measured in the fractions. Abs, absorbance.

(F-VYGG). The mature *S. carpocapsae* enzyme contains the catalytic triad (His57, Asp107 and Ser195) characteristic of the trypsin-like serine protease domain. The amino acids immediately flanking these active residues are also conserved. Seven cysteines can be identified in the primary sequence, three of which are, unusually, located at the C-terminal extension of the protease domain, excluding Cys191 and Cys220, which are highly conserved amino-acids in invertebrates and vertebrates. The amino acid residues Gly189, Gly216 and Thr226 appear to contribute to protease specificity for P1 small hydrophobic residues (Gudmundsdottir et al., 1996).

A sequence identity search in GenBank indicated that Sc-SP-3 exhibited high identity to several chymotrypsin-like sequences of organisms such as nematodes (25–30% identity), insects (29–30% identity) and vertebrates (27% identity) (Fig. 6).

3.4. Analysis and MALDI-TOF–MS identification of Sc-SP-3

The molecular mass of the purified protein was estimated to be about 30 kDa, and the p*I* was approximately 7. These values are close to those predicted for the protease encoded by *sc-sp-3*, with a molecular mass and p*I* of 28,900 Da and 6.4–6.9, respectively. N-terminal sequencing of the purified protease by Edman reaction resulted in the amino acid sequence VYGGQKARPGQFP, which was identified in the cDNA sequence of *sc-sp-3*. Moreover, peptide mass fingerprinting of the digested single spot obtained in 2D electrophoresis by MALDI-TOF–MS resulted in the identification of Sc-SP-3 with a significant score of 114 (scores greater than 75 are significant at $P < 0.05$), thus we conclude that the purified protein was encoded by the full-length *sc-sp-3* cDNA.

3.5. sc-sp-3 is exclusively expressed by the parasitic stage

sc-sp-3 expression was investigated by qRT-PCR at each stage of the nematode life cycle and showed that IJ in the arrested stage did not express *sc-sp-3*, but parasites inside the insect mid-gut, as well as those established in the haemocoel were transcribing the *sc-sp-3* gene. Fourth stage juveniles, adults, and first and second stage juveniles did not show significant expression of the protease (Fig. 7A). Although not significantly different, the amount of *sc-sp-3* expressed by nematodes still inside the gut was consistently higher than that expressed by nematodes in the haemocoel.

In in vitro assays, IJs began to express *sc-sp-3* at 6 h after induction with insect haemolymph (Fig. 7B).

3.6. Sc-SP-3 interaction with insect tissues

Sc-SP-3 activity in the host was investigated by feeding insect larvae and in an ex situ assay using insect mid-gut. Mid-gut of larvae that fed on Sc-SP-3 showed 24 h post-treatment evidence of histolysis with the lumen packed with cell debris, caused by the massive fragmentation of the epithelial cells and detachment from the basal lamina. The remaining epithelial cells lost the columnar shape and presented enlarged cavities. Identical signs were observed in tissues treated ex situ with 30 μg of Sc-SP-3 (Fig. 8). How this protease is able to affect proteins in epithelial tissues is shown by the extensive digestion observed either in tissue homogenates (Fig. 9A) or in extracellular proteins such as fibronectin, collagen and laminin (Fig. 9B), suggesting that it can be participating in the histolysis observed in treated mid-gut.

3.7. Sc-SP-3 causes cell death

Cytotoxic activity of Sc-SP-3 was investigated in cell cultures. The purified protein caused dose- and time-related mortality in *Sf*9 cell cultures, with an LD50 of 30 μg/ml (Fig. 10). More detailed assays showed that treated cells were evidencing nuclear condensation and fragmentation, which were increased in higher doses and with greater exposure time. DNA fragmentation was shown by DAPI and in agarose gels (Fig. 11A and B). Analysis of phosphatidylserine translocation showed early apoptosis in cells treated for

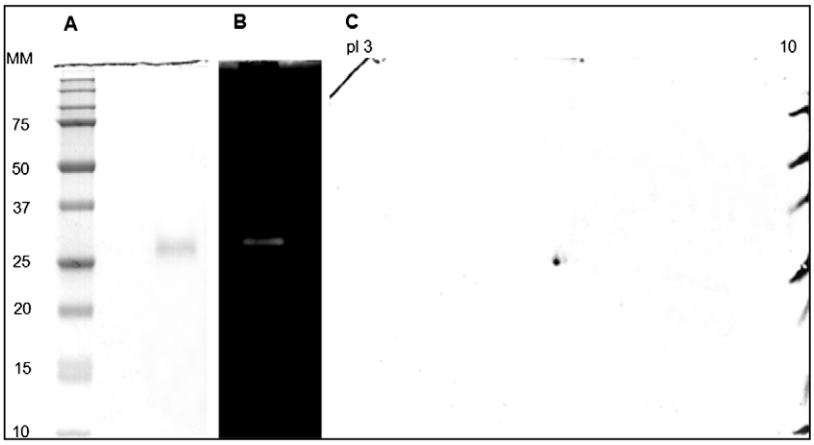

Fig. 3. Analysis of purified *Steinernema carpocapsae* serine protease-3 performed in SDS–PAGE (A), zymogram in a substrate of gelatine (B) and two-dimensional electrophoresis (C).

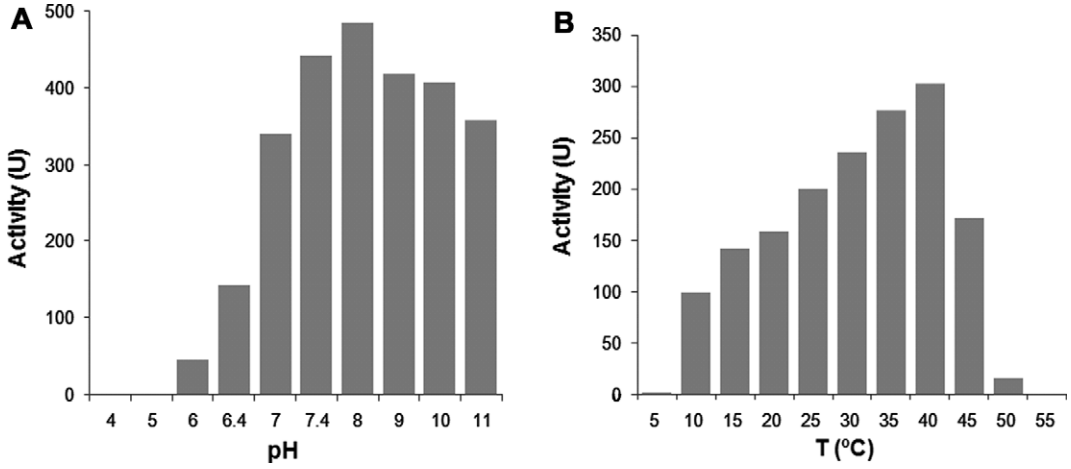

Fig. 4. The Optimal pH (A) and temperature (B) for *Steinernema carpocapsae* serine protease-3 activity tested against the specific substrate N-succinyl-Ala-Ala-Pro-Phe-pNA.

MRTLFVLFTFLVAASGVPLQDFAVPYVEQIFSEPARFPLDPEEFFRNLDQVNTTQFVYGGQKARP
GQFPQHAFMLTKKAKGFFICGASLLSPTHALTAAHCVEGIMAPSQIMAGGLNRRDRRAPNAQW
RSIHRATKPASYNSHTLLDDIAVVEFNPPMTLNRDVQLTKIVEDDAELLQEKKSYVTGFGTYTYKG
DQSVSSDELLWAEIDLFDFSRCQQLWDHGLWQKQICAGAKNLGAGPGDSGGPLQVLHEGTLF
QVGLTSYGTTDKFDDEFNQDRFPTVFTRVSSYCDFIAKVTDDAFTCSSLAQKPTVKPDCRF

Fig. 5. Amino acid sequences of *Steinernema carpocapsae* serine protease-3 with identification of the position of the putative signal peptide (discontinuous underlined), the N-terminal (continuous underline) and the active site residues (box).

6 h, whereas cells treated for 18 h demonstrated signs of final apoptosis (Fig. 12).

Caspase activation is a characteristic event of cells undergoing apoptosis, thus we check for the ability of Sc-SP-3 to induce caspase activation in treated *Sf*9 cells. The activation of caspases was done using a specific antibody against active caspase-3 that has been used previously to investigate lepidopteran active caspases (Vilaplana et al., 2007). Using this antibody we showed that *Sf*9 cells treated with 30 μg of Sc-SP-3 had caspase activation (Fig. 13 A). Evidence of activation of caspases was also measured in extracts of treated cells by monitoring the hydrolysis of DEVD-pNA, a substrate of *S. frugiperda* sf-caspase-1 (Aparna et al., 2003). Significant caspase activity was detected in cells treated with 30 μg of Sc-SP-3 and in positive control EGTA 50 mM (Fig. 13B). On the other hand, cells co-treated with the inhibitor of caspases z-VAD-fmk presented a low cleavage of DEVD-pNA caspase substrate (Fig. 13B) and a reduced nucleosomal cleavage visualised by DAPI (Fig. 13C). Identical observations were made in our positive control consisting of cells treated with the proapoptotic agent EGTA (50 mM) with z-VAD-fmk. Given that proteolytic activity of Sc-SP-3 was not inhibited by z-VAD-fmk (data not shown) we assume that Sc-SP-3 induces caspase-dependent apoptosis in insect cells.

4. Discussion

The participation of proteases in the parasitic process of *S. carpocapsae* was suggested by the fact that higher amounts of proteolytic activity are found in ESPs of virulent strains than in ESPs of less virulent strains. In this study, we purified and characterised a chymotrypsin-like protease (Sc-SP-3) obtained from

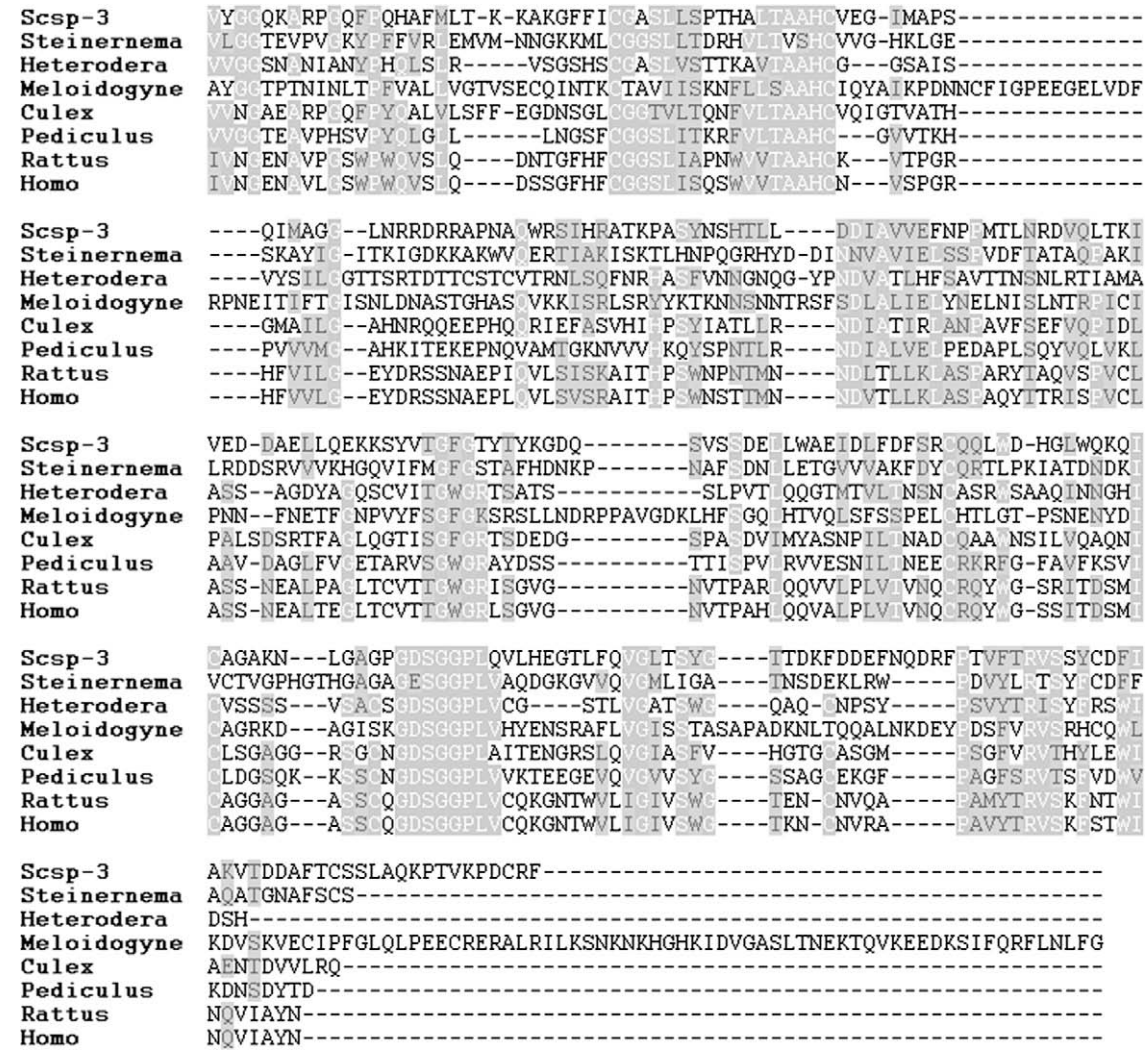

Fig. 6. *Steinernema carpocapsae* serine protease-3 alignment with known chymotrypsin-like serine proteases. Protein sequences were retrieved from GenBank and alignments performed using CLUSTAL W. Sequences begins at the first residue of the proposed mature proteins. Sequences compared were: *Steinernema carpocapsae* (AAT27470.1); *Heterodera glycines* (CAA74205.1); *Meloidogyne incognita* (AAV87529.1); *Culex quinquefasciatus* (XP001843365.1); *Pediculus humanus corporis* (AAX56335.1); and *Homo sapiens* (NP001898.1). Identical and similar amino acids are represented by dark and light grey, respectively.

ESPs of the parasitic stage of the entomopathogenic nematode of *S. carpocapsae*. Furthermore, we identified the full-length cDNA encoding the Sc-SP-3. Despite homology to other serine proteases, Sc-SP-3 has seven Cys residues, which is an unusual number and position. The mature Sc-SP-3 forms Cys42-Cys58 and Cys168-Cys182 disulphide bridges unlike most invertebrates that contain three disulphide bridges (Perona and Craik, 1995). The remaining three cysteine residues are located in a C-terminal domain with 53 residues that presents high homology with complement control protein (CCP). Brehm and Spiliotis (2008) suggested that parasites use CCP domain as targets to find suitable organs in the host.

The predicted mature catalytic domain of Sc-SP-3, substrate specificity and enzymatic inhibition of the purified protein allowed for its identification as a chymotrypsin-like serine protease. The N-terminal sequence of mature serine proteases is highly conserved. In mature proteins, the N-terminus is known to form a salt bridge with the well-conserved aspartic acid adjacent to the catalytic Ser195, thus stabilizing the active site (Perona and Craik, 1995; Hedstrom, 2002). The absence of the typically arginine or lysine residues at P-1 position restrain the activation by trypsin-like enzymes. Thus an autocatalytic mechanism is suggested, such as was proposed for other helminth serine proteases (Newport et al., 1988; Lilley et al., 1997). Indeed, serine proteases must be tightly regulated and sequestered to avoid damaging the cells or organisms that produced them.

sc-sp-3 is expressed by recovered IJs but not by the resistant stage or any other stage developing in the insect host. Moreover, parasitic nematodes still present inside the host gut are expressing more *sc-sp-3* than those already in the haemocoel, suggesting that Sc-SP-3 plays a role in the invasive process. The histolysis observed in mid-gut epithelial tissues in insects that had fed on Sc-SP-3 and in mid-gut tissues treated ex vivo with Sc-SP-3, clearly show that this protease has relevant activity in the host. These types of effects were also observed in larvae exposed to nematode infective juveniles (Simões et al., 2000). This finding supports our assumption that Sc-SP-3 is assisting nematode invasion via disruption of the mid-gut barrier, including cell detachment and fragmentation. Many parasitic nematodes excrete–secrete proteases that are hypothesised to be involved in invasion. For example, the serine protease secreted by the infective larvae of *Trichinella spiralis* was proposed to participate in parasitism by facilitating the movement of the larva via degradation of intra- and intercellular proteins (Romaris et al., 2002); and a metalloaminopeptidase and a

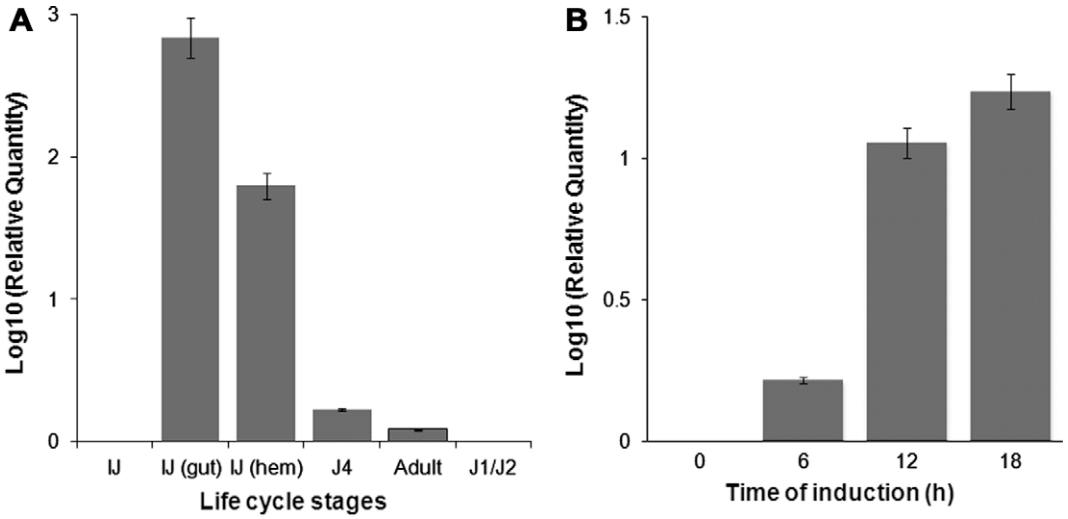

Fig. 7. *Steinernema carpocapsae* serine protease-3 expression analysis using quantitative real-time-PCR in the different nematode stages developing into the host (A) and after different times of induction in vitro with insect homogenates (B). IJ, infective juvenile (resistant stage); IJ (gut), infective juvenile collected from the gut; IJ (hem), infective juvenile collected from hemocoelium; J1, J2, J4, first, second and fourth stages.

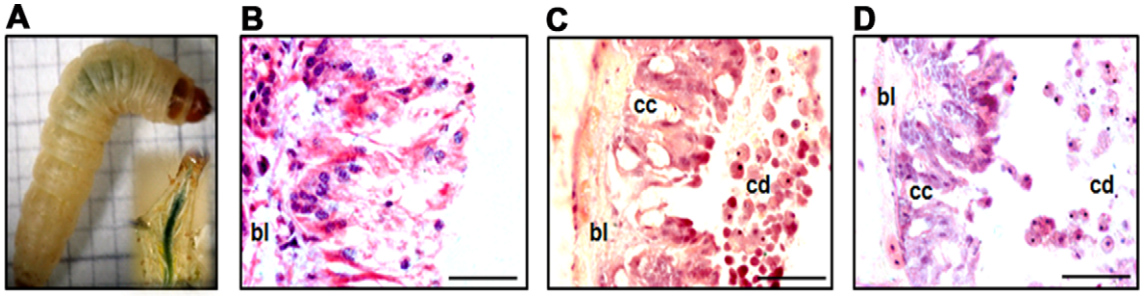

Fig. 8. Insect fed on blue stained diet with *Steinernema carpocapsae* serine protease-3 (Sc-SP-3) (A), mid-gut microphotographs of control larvae fed on agar plus PBS (B), of larvae fed on agar plus Sc-SP-3 (C) and of mid-gut treated ex vivo with Sc-SP-3 for 6 h (D). bl, basal lamina; cc, cell cavities; cd, cell debris. Bar represents 100 μm.

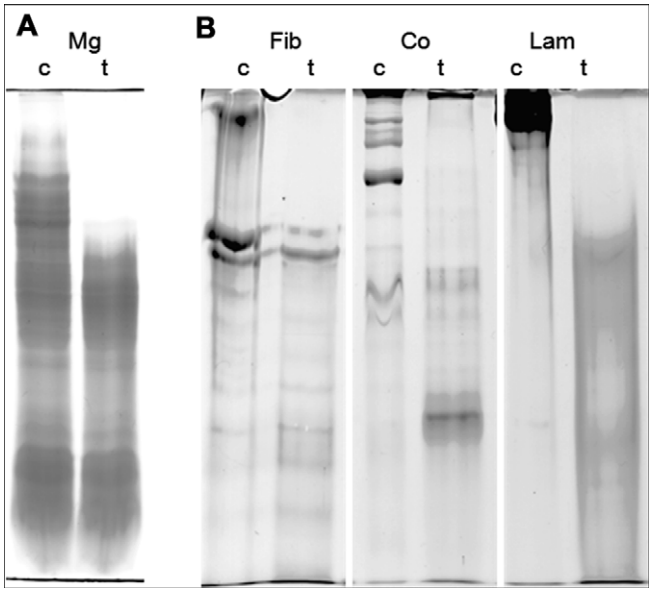

Fig. 9. SDS–PAGE of proteins extracted from mid-gut insect tissues (A) and of extracellular commercial proteins (B) control (PBS) and treated with *Steinernema carpocapsae* serine protease-3. c, control; Co, collagen; Fib, fibronectin; Lam, laminin; t, Sc-SP-3 treated.

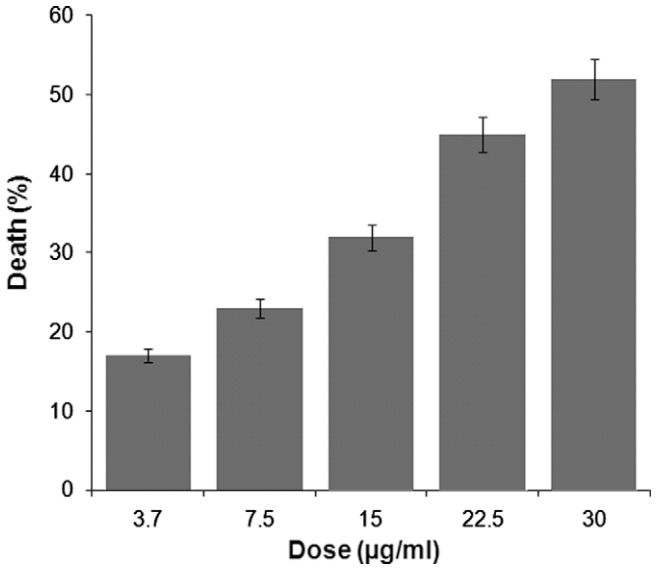

Fig. 10. Percentage of mortality of *Spodoptera frugiperda* (Insecta: Lepidoptera) cells (*Sf*9) in response to *Steinernema carpocapsae* serine protease-3 treatments.

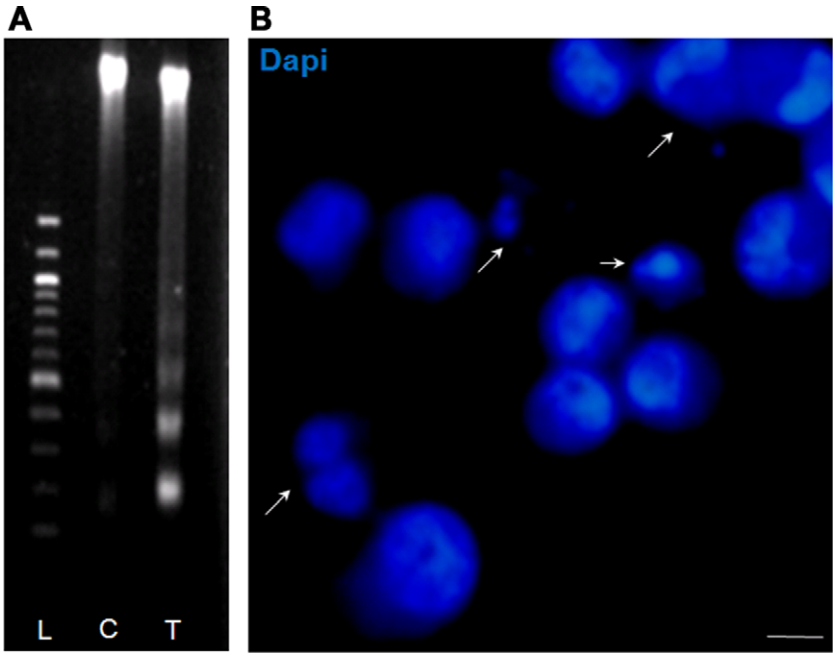

Fig. 11. DNA fragmentation in treated *Spodoptera frugiperda* (Insecta: Lepidoptera) cells (Sf9), as visualised by gel agarose electrophoresis (A) and DAPI (B). L, ladder; C, control; T, treated. Bar represents 7 μm.

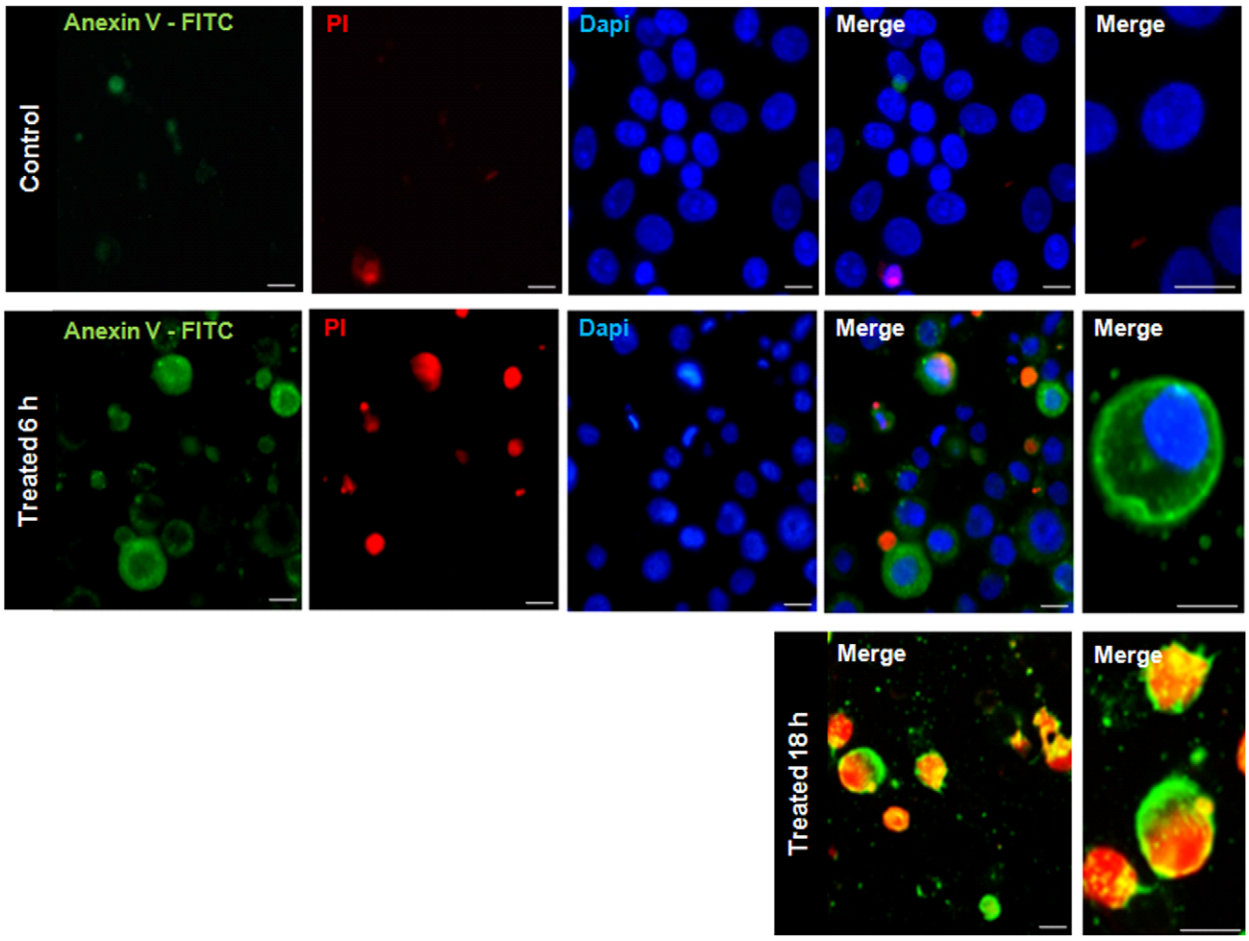

Fig. 12. Early and late apoptosis in *Spodoptera frugiperda* (Insecta: Lepidoptera) cells (Sf9) treated with *Steinernema carpocapsae* serine protease-3 for 6 and 18 h as shown with annexin-V–FITC staining. Bar represents 7 μm.

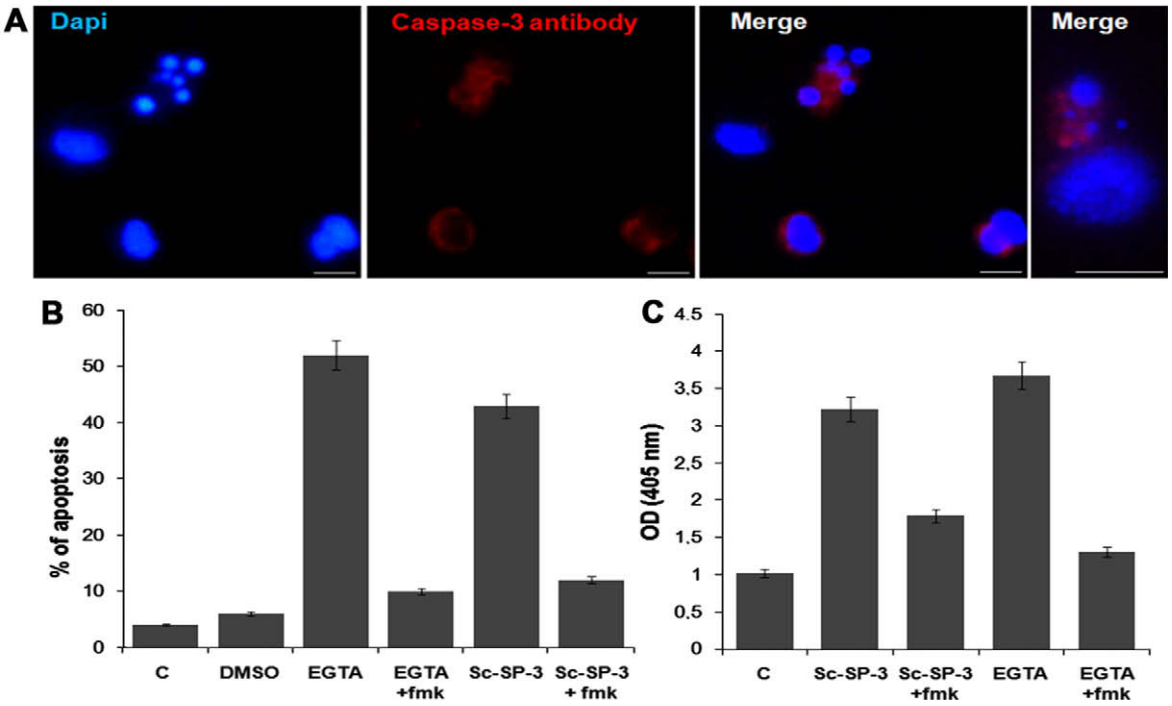

Fig. 13. Activation of caspases in *Spodoptera frugiperda* (Insecta: Lepidoptera) cells (Sf9) treated with *Steinernema carpocapsae* serine protease-3 (Sc-SP-3). Activity in cells treated for 18 h measured with anti-active caspase-3 (A); percentage of apoptotic Sf9 cells in control and in treatments with DMSO, EGTA, EGTA plus cell-permeable caspase inhibitor N-benzyloxycarbonyl-Val-Ala-Asp(O-Me) fluoromethyl ketone (z-VAD-fmk), Sc-SP-3 and Sc-SP-3 plus Z-VAD-cmk, measured by DAPI (B); hydrolysis of N-Acetyl-Asp-Glu-Val-Asp *p*-nitroanilide (DEVD-pNA) in cells under the conditions referred in B (C). Bar represents 7 μm.

trypsin-like serine protease produced by *Anisakis simplex* larvae were suggested to allow invasion and penetration of the host stomach and intestinal wall, by promoting the degradation of host tissue macromolecules (Sakanari and McKerrow, 1990). Degradation of host proteins has also been attributed to other secreted proteases, such as the cysteines of *H. contortus*, which are capable of degrading albumin and fibrinogen in host blood (Knox et al., 1993), and the serine, cysteine and metalloproteases of *T. spiralis* adults that have collagenolytic and elastolytic activities (Todorova, 2000).

The mechanism involved in the tissue destruction caused by Sc-SP-3 is far from being decrypted, however, it was clear that this protease was able to hydrolyse cell matrix proteins and to cause cell death. Assays in vitro using cells of a nematode natural host (*Sf*9) showed that Sc-SP-3 induces dose-dependent cell mortality, with cells presenting nuclear fragmentation and phosphatidylserine translocation, which are characteristic signs of apoptosis. These cells also presented activated caspases shown by the use of an antibody against active caspase-3 and by the hydrolysis of DEVD caspase substrate. Moreover the inhibition of caspases by the caspase inhibitor z-VAD-fmk caused the decrease of cellular death. These findings suggested that cell mortality induced by Sc-SP-3 was caspase-dependent. Apoptosis-inducing factors were also referenced in *N. brasiliensis*, *T. spiralis* and *T. pseudospiralis* ESPs that induce cell apoptosis through the extrinsic apoptotic pathway (Boonmars et al., 2005; Kuroda et al., 2002; Wu et al., 2005).

A detailed knowledge of the molecular effectors of the pathogenic process engendered by the entomopathogenic nematode *S. carpocpasae* is essential to understanding the virulence of this nematode, as well as for eventual use of expressed entomotoxins. A first step is accomplished by the characterisation of Sc-SP-3, the identification of the encoding cDNA and the demonstration of its activity in insect invasion. Further information on the toxicity, specificity and mode of action of this protein in insects, together with its safety to other organisms, is needed to evaluate its viability as an insecticidal compound.

Acknowledgements

Our thanks go to Fundação para a Ciência e Tecnologia (FCT, P) and Fundação Lusa Americana para o Desenvolvimento (FLAD, P) that funded this work (Projects POCTI/BSE/41630/2001 and 223/06). FCT also supported fellows to D.T. (SFRH/BD/18986/2004), M.L.R. (SFRH/BPD/15324/2005), R.M. (SFRH/BPD/32473/2006), G.C. (SFRH/BD/14387/2003) and G.N. (POCI/AGR/56300/2004).

References

Aparna, G., Bhuyan, K., Sahdev, S., Hasnain, E., Kaufman, J., Ramaiah, A., 2003. Stress-induced apoptosis in *Spodoptera frugiperda* (*Sf*9) cells: baculovirus p35 mitigates eIF2R phosphorylation. Biochemistry 42, 15352–15360.

Bedding, R.A., 1984. Long scale production, storage and transport of the insect parasitic nematodes *Neoaplectana* spp. and *Heterorhabditis* spp.. Ann. Appl. Biol. 104, 117–120.

Berasain, P., Goni, F., McGonigle, S., Dowd, A., Dalton, J.P., Frangione, B., Carmona, C., 1997. Proteinases secreted by *Fasciola hepatica* degrade extracellular matrix and basement membrane components. J. Parasitol. 83, 1–5.

Boemare, N., Laumond, C., Luciani, J., 1982. Mise en évidence d'une toxicogenése provoquée par le nematode axénique entomophage *Neoaplectana carpocapsae* Weiser chez l'insect axénique *Galleria mellonella*. C. R. Acad. Sci. D 295, 543–546.

Boonmars, T., Wu, Z., Nagano, I., Takahashi, Y., 2005. What is the role of p53 during the cyst formation of *Trichinella spiralis*? A comparable study between knockout mice and wild type mice. Parasitology 131, 705–712.

Brehm, K., Spiliotis, M., 2008. The influence of host hormones and cytokines on *Echinococcus multilocularis* signalling and development. Parasite 15, 286–290.

Burman, M., 1982. *Neoaplectana carpocapsae*: toxin production by axenic insect parasitic nematodes. Nematologica 28, 62–70.

Caldas, C., Pereira, A., Cherqui, A., Simões, N., 2002. Purification and characterization of an extracellular protease from *Xenorhabdus nematophila* involved in insect immunosupression. Appl. Environ. Microbiol. 68, 1297–1304.

Chen, L., Rao, K.V., He, Y.X., Ramaswamy, K., 2002. Skin-stage schistosomula of *Schistosoma mansoni* produce an apoptosis-inducing factor that can cause apoptosis of T cells. J. Biol. Chem. 277, 34329–34335.

Cliffe, L.J., Potten, C.S., Booth, C.E., Grencis, R.K., 2007. An increase in epithelial cell apoptosis is associated with chronic intestinal nematode infection. Infect. Immun. 75, 1556–1564.

Cruz, N., Rosa, J.S., Simões, N., 2001. Encapsulation response of 6th instar of *Pseudaletia unipuncta* (Lepidoptera: Noctuidae) to *Steinernema carpocapsae* (Nematoda: Steinernematidae). J. Invertebr. Pathol. 78, 272–274.

Else, K.J., 2005. Have gastrointestinal nematodes outwitted the immune system? Parasite Immunol. 27, 407–415.

Forst, S., Clarke, D.J., 2002. Nematode-bacterium symbiosis. In: Gaugler, R. (Ed.), Entomopathogenic Nematodes. CABI Publishing, Wallingford, pp. 57–77.

Götz, P., Boman, A., Boman, H.G., 1981. Interaction between insect immunity and an insect-pathogenic nematode with symbiotic bacteria. Proc. R. Soc. Lond. 212, 333–350.

Gudmundsdottir, E., Spilliaert, R., Yang, Q., Craik, C.S., Bjarnason, J.B., Gudmunds&ttir, A., 1996. Isolation and characterization of two cDNAs from Atlantic cod encoding two distinct psychrophilic elastases. Comp. Biochem. Physiol. B Biochem. Mol. Biol. 113, 795–801.

Hedstrom, L., 2002. Serine protease mechanism and specificity. Chem. Rev. 102, 4501–4523.

James, E.R., Green, D.R., 2004. Manipulation of apoptosis in the host–parasite interaction. Trends Parasitol. 20, 280–287.

Jenson, J.S., O'Connor, R., Osborne, J., Devaney, E., 2002. Infection with *Brugia microfilariae* induces apoptosis of CD4(+) T lymphocytes: a mechanism of immune unresponsiveness in filariasis. Eur. J. Immunol. 32, 858–867.

Kaya, H.K., Gaugler, R., 1993. Entomopathogenic nematodes. Ann. Rev. Entomol. 38, 181–206.

Knox, D.P., Redmond, D.L., Jones, D.G., 1993. Characterization of proteinases in extracts of adult *Haemonchus contortus*, the ovine abomasal nematode. Parasitology 106, 395–404.

Kuroda, A., Uchikawa, R., Matsuda, S., Yamada, M., Tegoshi, T., Arizono, N., 2002. Up-regulation of Fas (CD95) and induction of apoptosis in intestinal epithelial cells by nematode-derived molecules. Infect. Immun. 70, 4002–4008.

Laemmli, U.K., 1970. Cleavage of structural proteins during assembly of the head of bacteriophage T4. Nature 227, 680–685.

Laumond, C., Simões, N., Boemare, N., 1989. Toxins of entomoparasitic nematodes. Pathogenicity of *Steinernema carpocapsae* – prospectives of genetic engineering. C. R. Acad. Agric. France 75, 135–138.

Lilley, C.J., Urwin, P.E., Atkinson, H.J., McPherson, M.J., 1997. Characterization of cDNAs encoding serine proteinases from the soybean cyst nematode *Heterodera glycines*. Mol. Biochem. Parasitol. 89, 195–207.

McKerrow, J.H., Jones, P., Sage, H., Pino-Heiss, S., 1985. Proteinases from invasive larvae of the trematode parasite *Schistosoma mansoni* degrade connective tissue and basement-membrane macromolecules. J. Biochem. 231, 47–51.

Neuhoff, V., Arold, N., Taube, D., Ehrhardt, W., 1988. Improved staining of proteins in polyacrylamide gels including isoelectric focusing gels with clear background at nanogram sensitivity using Coomassie brilliant blue G-250 and R-250. Electrophoresis 9, 255–262.

Newport, G.R., McKerrow, J.H., Hedstrom, R., Pettit, M., McGarrigle, L., Barr, P.J., Agabian, N., 1988. Cloning of the proteinase that facilitates infection by schistosome parasites. J. Biol. Chem. 263, 13179–13184.

Nielsen, H., Engelbrecht, J., Brunak, S., von Heijne, G., 1997. Identification of prokariotic and eukariotic signal peptides and prediction of their cleavage sites. Protein Eng. 10, 1–6.

Peters, A., Ehlers, R., 1997. Encapsulation of the Entomopathogenic Nematode *Steinernema feltiae* in *Tipula oleracea*. J. Invertebr. Pathol. 69, 218–222.

Perona, J.J., Craik, C.S., 1995. Structural basis of substrate specificity in the serine proteases. Protein Sci. 4, 337–360.

Rahman, M.M., McFadden, G., 2006. Modulation of tumor necrosis factor by microbial pathogens. PLoS Pathog. 2 (2), e4.

Redmond, D.L., Knox, D.P., Newlands, G., Smith, W.D., 1997. Molecular cloning and characterization of a developmentally regulated putative metallopeptidase present in a host protective extract of *Haemonchus contortus*. Mol. Biochem. Parasitol. 85, 77–87.

Romaris, F., North, S.J., Gagliardo, L.F., Butcher, B.A., Ghosh, K., Beiting, D.P., Panico, M., Arasu, P., Dell, A., Morris, H.R., Appleton, J.A., 2002. A putative serine protease among the excretory–secretory glycoproteins of L1 *Trichinella spiralis*. Mol. Biochem. Parasitol. 122, 149–160.

Sakanari, J.A., McKerrow, J.H., 1990. Identification of the secreted neutral proteases from *Anisakis simplex*. J. Parasitol. 76, 625–630.

Sergeant, M., Jarrett, P., Ousley, M., Morgan, J.A., 2003. Interactions of insecticidal toxin gene products from *Xenorhabdus nematophilus* PMFI 296. Appl. Environ. Microbiol. 69, 3344–3349.

Simões, N., Caldas, C., Rosa, J.S., Bonifassi, E., Laumond, C., 2000. Pathogenicity caused by high virulent and low virulent strains of *Steinernema carpocapsae* to *Galleria mellonella*. J. Invertebr. Pathol. 75, 47–54.

Smith, A.M., Dalton, J.P., Clough, K.A., Kilbane, C.L., Harrop, S.A., Hole, N., Brindley, P.J., 1994. Adult *Schistosoma mansoni* express cathepsin L proteinase activity. Mol. Biochem. Parasitol. 67, 11–19.

Thaler, J.O., Duvic, B., Givaudan, A., Boemare, N., 1998. Isolation and entomotoxic properties of the *Xenorhabdus nematophilus* F1 lecithinase. Appl. Environ. Microbiol. 64, 2367–2373.

Todorova, V.K., 2000. Proteolytic enzymes secreted by larval stage of the parasitic nematode *Trichinella spiralis*. Folia Parasitol. 40, 141–145.

Trap, C., Boireau, P., 2000. Proteases in helminthic parasites. Vet. Res. 31, 461–471.

Vilaplana, L., Pascual, N., Perera, N., Belle, X., 2007. Molecular characterization of an inhibitor of apoptosis in the Egyptian armyworm, *Spodoptera littoralis*, and midgut cell death during metamorphosis. Insect Biochem. Mol. Biol. 37, 1241–1248.

Wang, Y., Gaugler, R., 1999. *Steinernema glaseri* surface coat proteins supresses the immune response of *Popillia japonica* (Coleoptera: Scarabaeidae) larvae. Biol. Control 14, 45–50.

White, A.C., Molinari, J.L., Pillai, A.V., Rege, A.A., 1992. Detection and preliminary characterization of *Taenia solium* metacestode proteases. J. Parasitol. 78, 281–287.

Wong, J.Y., Harrop, S.A., Day, S.R., Brindley, P.J., 1997. Schistosomes express two forms of cathepsin D. Biochim. Biophys. Acta 1338, 156–160.

Wu, Z., Nagano, I., Boonmars, T., Takahashi, Y., 2005. Tumor necrosis factor receptor-mediated apoptosis in *Trichinella spiralis*-infected muscle cells. Parasitology 131, 373–381.